Article

Cell Reports

Individual Human Cytotoxic T Lymphocytes Exhibit Intraclonal Heterogeneity during Sustained Killing

Graphical Abstract

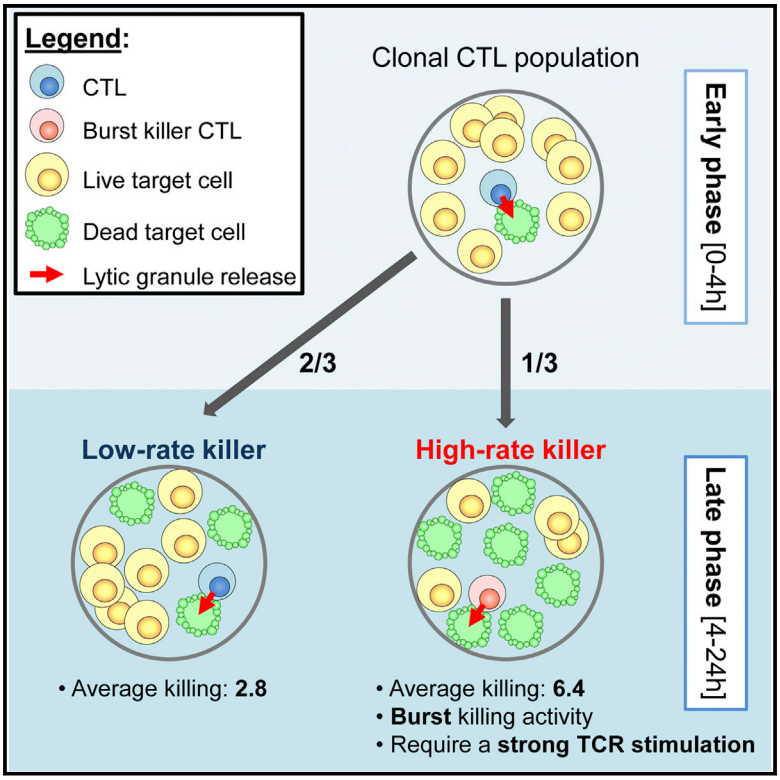

Highlights

- Sustained killing activity allows CTLs to control an excess of target cells
- The multiple killing performance of individual CTLs is highly heterogeneous
- High-rate killing is delayed in time and requires strong antigenic stimulation

Authors

Zilton Vasconcelos, Sabina Müller, ..., Salvatore Valitutti, Loïc Dupré

Correspondence

salvatore.valitutti@inserm.fr (S.V.), loic.dupre@inserm.fr (L.D.)

In Brief

Cytotoxicity is viewed as a rapid and homogeneous response of CTLs to antigen-bearing target cells. Vasconcelos et al. report that human CTL clones are endowed with a sustained cytotoxic activity when facing an excess of target cells. Such activity relies on a high heterogeneity of individual CTL killing performances, whereby only a subset of high-rate killer CTLs develop with time. The authors propose that these CTL traits are key to the calibration of cytotoxic responses.

Vasconcelos et al., 2015, Cell Reports *11*, 1474–1485
June 9, 2015
http://dx.doi.org/10.1016/j.celrep.2015.05.002

OPEN ACCESS
CellPress

Cell Reports
Article

Individual Human Cytotoxic T Lymphocytes Exhibit Intraclonal Heterogeneity during Sustained Killing

Zilton Vasconcelos,[1,2,3,4] Sabina Müller,[1,2,3] Delphine Guipouy,[1,2,3] Wong Yu,[5] Claire Christophe,[2,6] Sébastien Gadat,[7] Salvatore Valitutti,[1,2,3,8,*] and Loïc Dupré[1,2,3,8,*]

[1]INSERM, UMR 1043, Centre de Physiopathologie de Toulouse Purpan, 31300 Toulouse, France
[2]Université Toulouse III Paul-Sabatier, 31062 Toulouse, France
[3]CNRS, UMR 5282, 31300 Toulouse, France
[4]Fernandes Figueira Institute, Fiocruz, 22250-020 Rio de Janeiro, Brazil
[5]Department of Microbiology and Immunology, Stanford University School of Medicine, Stanford, CA 94305, USA
[6]Institut de Mathématiques de Toulouse, UMR 5219, 31062 Toulouse, France
[7]Toulouse School of Economics, Université Toulouse I Capitole, 31000 Toulouse, France
[8]Co-senior author
*Correspondence: salvatore.valitutti@inserm.fr (S.V.), loic.dupre@inserm.fr (L.D.)
http://dx.doi.org/10.1016/j.celrep.2015.05.002

SUMMARY

The killing of antigen-bearing cells by clonal populations of cytotoxic T lymphocytes (CTLs) is thought to be a rapid phenomenon executed uniformly by individual CTLs. We combined bulk and single-CTL killing assays over a prolonged time period to provide the killing statistics of clonal human CTLs against an excess of target cells. Our data reveal efficiency in sustained killing at the population level, which relied on a highly heterogeneous multiple killing performance at the individual level. Although intraclonal functional heterogeneity was a stable trait in clonal populations, it was reset in the progeny of individual CTLs. In-depth mathematical analysis of individual CTL killing data revealed a substantial proportion of high-rate killer CTLs with burst killing activity. Importantly, such activity was delayed and required activation with strong antigenic stimulation. Our study implies that functional heterogeneity allows CTL populations to calibrate prolonged cytotoxic activity to the size of target cell populations.

INTRODUCTION

The major mechanism by which cytotoxic T lymphocytes (CTLs) kill specific target cells relies on the secretion of lytic molecules contained in specialized granules. Upon antigen recognition at the surface of target cells, CTLs assemble a lytic synapse that allows stable adhesion and secretion of lytic molecules (Dustin and Long, 2010). Lethal hit delivery can occur within a few minutes after the initial contact between CTLs and target cells (Poenie et al., 1987), and in addition, it is triggered at antigen concentrations much lower than those required for full activation and cytokine production (Faroudi et al., 2003; Purbhoo et al., 2004; Valitutti et al., 1996). Another distinct feature of CTLs is their propensity to kill multiple target cells (Macken and Perelson, 1984; Perelson and Bell, 1982; Rothstein et al., 1978), either simultaneously or serially by bouncing from one target cell to another (Wiedemann et al., 2006). Together, the above reported CTL features contributed to put forth the notion that CTL-mediated cytotoxicity is a binary response, rapidly elicited via the release of small lytic quanta, sufficient to annihilate individual target cells.

Recent studies have brought to light the concept that during the activation of naive $CD8^+$ T lymphocyte populations, individual precursors display heterogeneous responses in terms of expansion rate and differentiation (Beuneu et al., 2010; Buchholz et al., 2013; Gerlach et al., 2013), with diversification occurring both at interclonal and intraclonal levels (Lemaître et al., 2013). Rather than being a source of inconsistent T cell responses, heterogeneous individual behaviors appear to give rise to robust T cell responses at a population level by an averaging process (Buchholz et al., 2013).

In this context, we asked what level of heterogeneity individual $CD8^+$ T cells might display in their cytotoxic function. This question can be best addressed by studying CTL multiple killing capability in conditions in which individual CTLs are challenged by an excess of target cells. CTL killing efficiency is usually evaluated by measuring the percentage of dead target cells resulting from a 4-hr incubation with CTLs at a relatively high cell density and effector to target (E:T) ratio (Thorn and Henney, 1976; Zeijlemaker et al., 1977). Although useful in estimating and comparing the killing potential of different CTL populations, the conventional assays fail to consider individual CTL behavior.

We developed here a combination of flow-cytometry- and microscopy-based assays to provide kinetic measurements of target cell elimination by individual human CTLs belonging to clonal populations. Our data reveal that CTLs are endowed with a previously unappreciated ability to control an excess of target cells over prolonged time frames. Individual CTLs were able to eliminate up to 12 target cells in 12 hr. However, the contribution of individual CTLs to the control of target cells was very heterogeneous. A similar variability of individual killing performance was measured in different clones. In-depth statistical analysis revealed that within a clone, only a subset of CTLs

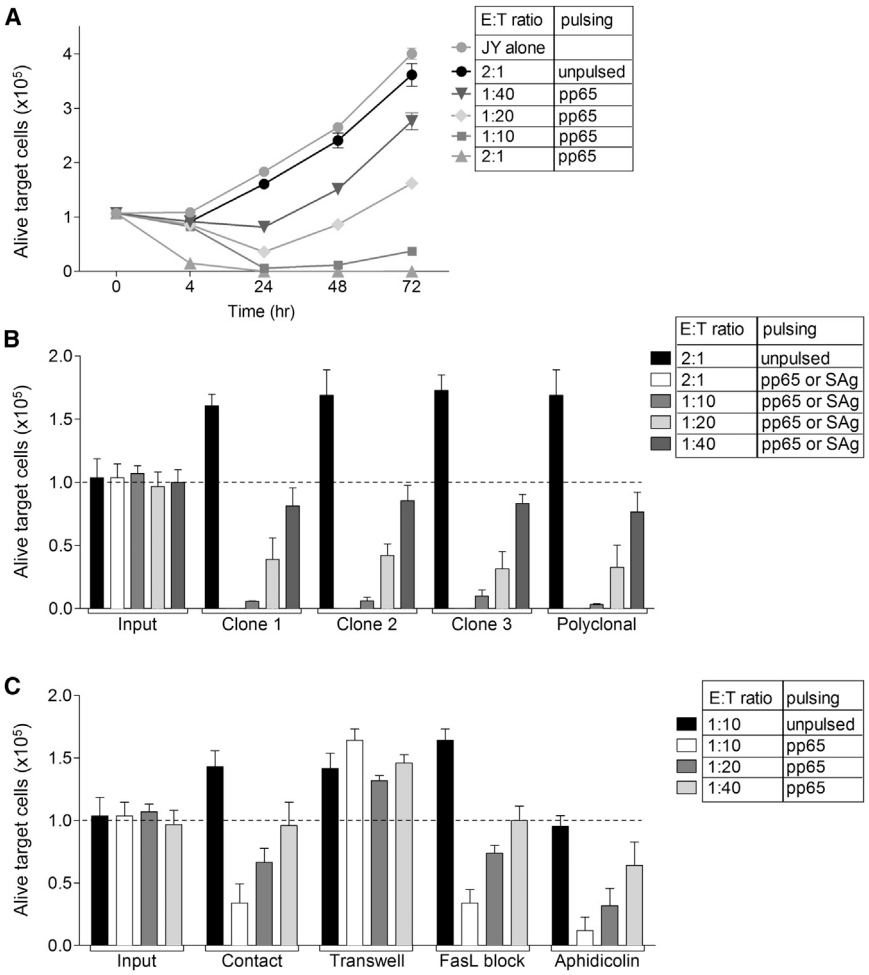

Figure 1. CTLs Control an Excess of Target Cells over Prolonged Time Periods

JY cells (targets) were pulsed with 100 nM pp65 or left unpulsed and were then seeded at 100,000 cells together with different numbers of CTLs (effectors, at E:T ratios of 2:1, 1:10, 1:20, and 1:40).

(A) Absolute counts of residual live target cells (see Figure S1 for a description of methods) after 4-, 24-, 48-, and 72-hr co-culture with CTLs at the indicated ratios.

(B) Absolute counts of residual live target cells after 24-hr co-culture with three different CTL clones and a polyclonal $CD8^+$ T cell line.

(C) Absolute counts of residual live target cells after 24 hr under the following conditions: direct contact with CTLs (as in A and B), separated from stimulated CTL via a transwell, treated with an anti-FasL blocking antibody, and treated with aphidicolin.

All graphical values represent the mean ± SD of triplicates from one representative experiment out of six performed. See also Figure S1.

displayed a high-rate killing capability. This subset developed upon contact with the target cells, required a strong T cell receptor (TCR)-mediated CTL activation, and displayed a burst kinetic behavior. Rather than being imprinted, such behavior was reset in the progeny of individual cells. Together, our data reveal that the cytotoxic activity of human CTLs is a cumulative process. It results from the heterogeneous multiple killing capacity of individual CTLs and from the delayed onset of a burst killing activity in a subset of CTLs. Such a process might allow CTLs to calibrate their global responses to various and heterogeneous target cell populations.

RESULTS

CTLs Control an Excess of Target Cells over Prolonged Time Periods

To investigate the killing potential of CTLs at low E:T ratios, we employed HLA-A2-restricted human CTL clones specific for the cytomegalovirus (CMV) pp65 peptide NLVPMVATV presented by HLA-A2-matched Epstein-Barr virus (EBV)-transformed B cells (JY). The impact of CTL on target cells was assessed by counting, over time, the remaining number of live target cells using beads as an internal reference (Figures S1A and S1B). When 100,000 peptide-pulsed target cells were incubated at a 2:1 E:T ratio, 15,020 target cells were found alive after 4 hr and only 1,833 after 24 hr (Figure 1A). Live target cells could no longer be detected at 48 and 72 hr, indicating that they had been fully eliminated. Unexpectedly, at a 1:10 E:T ratio, although 82,419 cells were still alive after 4 hr, only 5,854 target cells were found alive after 24 hr, implying that the outnumbered CTLs killed multiple target cells over this period. At later time points, moderate target cell growth was detected, indicating that the complete elimination of target cells was not reached at this ratio. At the 1:20 and 1:40 E:T ratios, a transient control of target cell number was observed at 24 hr, followed by an outgrowth of target cells. In control conditions, unpulsed target cells expanded over time to reach 361,250 cells after 72 hr, independently of the presence of CTL. We then compared the efficiency of different CMV-specific CTL clones at controlling target cell populations at low E:T ratios. The three clones tested exhibited a similar capability to control target cells over 24 hr (Figure 1B). This also applied to a polyclonal CTL line reacting to a cocktail of super-antigens presented by the same target cells, suggesting a very homogenous killing efficiency among effector CTL populations. The observed impact of outnumbered CTLs on target cells might operate via a contact-dependent cytotoxicity or via the release of soluble factors with cytotoxic or cytostatic effects. To test this latter possibility, CTLs were activated by peptide-pulsed cells in the upper well of a transwell (2:1 E:T ratio) and additional cells were placed in the lower well as targets. The survival of these cells was unaffected, indicating that in our model, the control exerted by CTLs requires either a contact or a proximity that was lost in the transwell

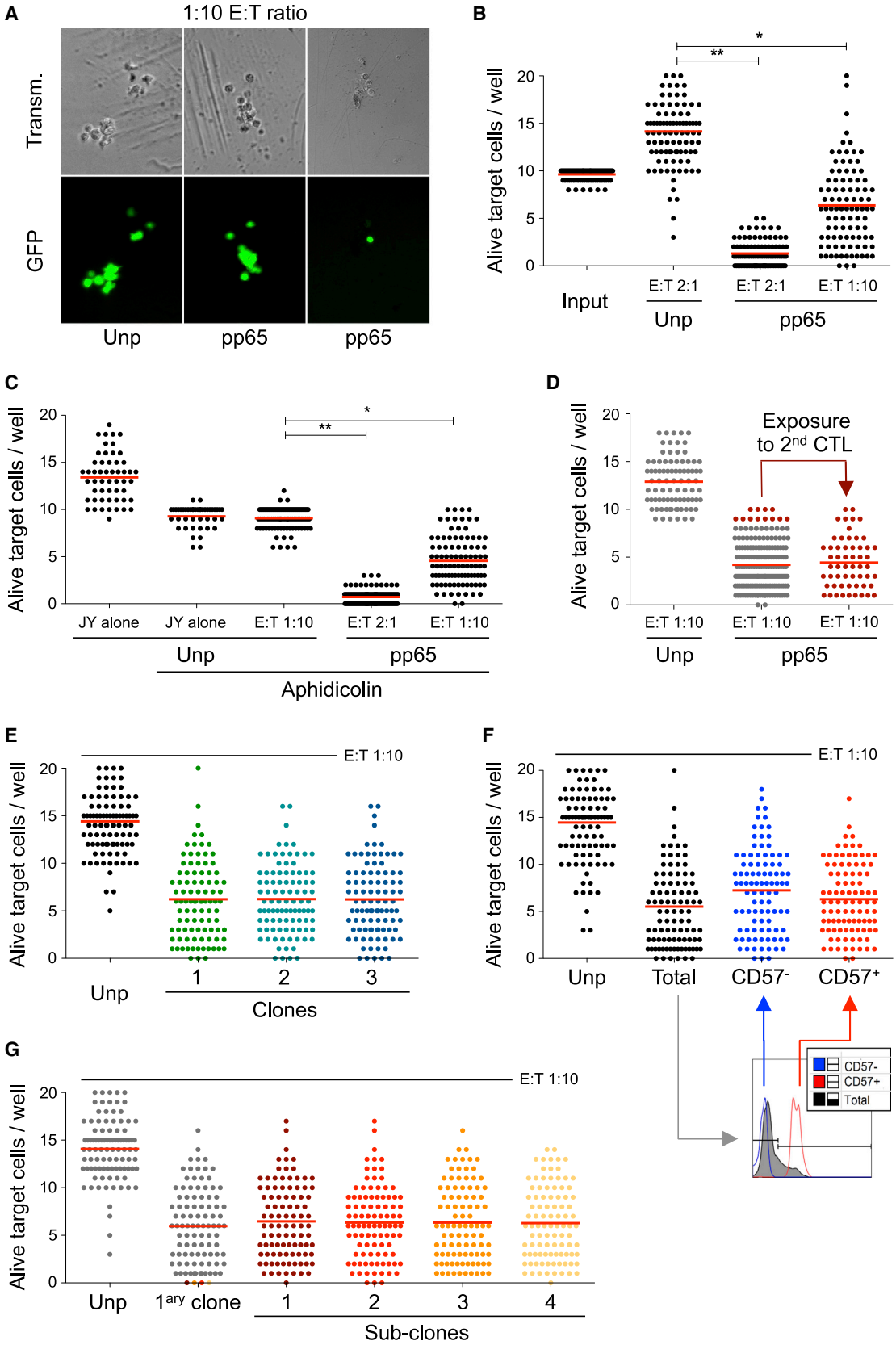

(legend on next page)

system (Figure 1C). To discriminate between the Fas-L and perforin/granzyme B pathways, we blocked Fas-L with a specific antibody. The fact that this treatment did not alter the activity of CTLs in controlling the target cells implies that the observed effects are dependent on the perforin/granzyme B pathway. Cell-cycle blockage with aphidicolin resulted in an improvement of target cell control by the outnumbered CTLs, showing that at low E:T ratios, the expansion of residual target cells partly counteracts the global effect of CTLs. In conclusion, the above results show that a small number of CTLs can control a large excess of target cells over prolonged time frames, revealing that populations of human effector CTLs share a remarkably high multiple killing capacity.

Intraclonal Heterogeneity in Multiple Killing Efficiency by Individual CTLs

We then asked whether individual CTLs comprising a clonal population contributed equivalently to killing. We developed a cell-sorter-assisted approach, whereby ten GFP-expressing target cells were exposed to a single CTL. After 24 hr, the number of residual alive target cells was evaluated by counting GFP-positive cells by microscopy. Indeed, our preliminary experiments showed that GFP expression was lost by dead cells (Figure S2). In control wells containing 20 CTLs and 10 pulsed target cells, most target cells were eliminated after 24 hr, confirming our previous observation in bulk assays and indicating that our miniaturized assay did not hinder killing activity (Figures 2A and 2B). When the ten target cells were exposed to a single CTL, a broad distribution in the number of residual live target cells was measured in the different wells, suggesting a very heterogeneous ability of individual CTLs to eliminate multiple target cells. Heterogeneity in residual live target cells could however be related to differential target cell expansion among wells, as observed in wells containing unpulsed target cells. To rule out this possibility, we performed single-CTL assays in the presence of aphidicolin to block the target cell cycle. Under this condition, although the expansion of GFP-expressing target cells was prevented, most of the heterogeneity in residual live target cells was maintained (Figure 2C). We next challenged the possibility that the observed heterogeneity might be related to the uneven distribution among wells of target cells with distinct susceptibility to CTL attack. To this end, wells containing nine or ten live target cells after incubation with a first CTL were re-exposed to a second CTL. Heterogeneous numbers of residual live target cells were counted from well to well, indicating that target cells surviving the first CTL were not intrinsically resistant to CTL attack (Figure 2D). These data demonstrate that, although most individual CTLs derived from a particular effector clone contribute to killing over a 24-hr time window, their efficiency in killing multiple target cells is highly heterogeneous.

We then addressed whether heterogeneity in multiple killing efficiency might be distinct from one CTL clone to another. In the three pp65-specific clones tested, very similar multiple killing heterogeneity was measured, as indicated by the range in the number of residual live target cells (Figure 2E). The observed killing heterogeneity might be linked to some degree of diversification of individual CTLs comprising a clone. Analysis of CD45RO, CCR7, CD27, CD28, IL7Rα, PD-1, and perforin expression showed that individual CTLs uniformly belonged to the effector memory stage (Figure S3). In contrast, CD57, a marker of terminally differentiated CTLs associated with reduced proliferation and killing potential, was expressed with some level of heterogeneity. To test whether CD57 expression might be related to multiple killing efficacy, individual $CD57^+$ and $CD57^-$ CTLs were sorted and exposed to ten target cells (Figure 2F). A comparable multiple killing activity was observed in each subset, reproducing the killing-rate heterogeneity observed in the unsorted CTLs. We next asked whether the multiple killing activity of an individual CTL might be transmitted to its progeny. To that aim, we expanded individual CTLs that had been shown to eliminate ten target cells in the single-CTL killing assay. When exposed to ten target cells, the progeny of such multiple killers reproduced the individual cell heterogeneity previously observed (Figure 2G). Taken together, the above results show that different clones exhibit a similar intraclonal heterogeneity in multiple killing. They also reveal that this heterogeneity is reset in the progeny of individual CTLs.

Analysis of CTL Killing Kinetics Identifies High-Rate and Low-Rate Killer Cells

To first evaluate the kinetics of CTL multiple killing, we monitored the occurrence of killing events over 12 hr by detecting

Figure 2. Intraclonal Heterogeneity in Multiple Killing Capacity by Individual CTLs

GFP-expressing target JY cells, pulsed with 100 nM pp65 or left unpulsed, were seeded with a cell sorter at ten cells per well in U-bottom 96-well plates in the presence of a single CTL (E:T ratio 1:10) or 20 CTLs (E:T ratio 2:1). Wells were examined by fluorescence microscopy after 24-hr co-culture to count the number of residual GFP-positive cells.

(A) Representative 10× magnification images of wells initially containing one CTL and either ten unpulsed target cells (left panels) or ten pp65 pulsed target cells (middle and right panels).

(B) Counts of GFP-positive cells in individual wells at input and following 24-hr co-culture with CTLs under the indicated pulsing and ratio conditions. Each dot represents a well, while the bar represents the mean of 96 wells per condition. The p values are results of t tests between the indicated conditions (*$p < 0.05$; **$p < 0.001$). One representative experiment out of four is presented.

(C) Counts of GFP-positive cells in individual wells following 24-hr co-culture with CTLs in the presence of aphidicolin, which was used to prevent target cell division. One representative experiment out of three is presented.

(D) Following an initial 24-hr co-culture, wells in which the ten target cells had best resisted the single CTL (and still contained nine or ten GFP-positive cells) were re-exposed for 24 hr to a new CTL (re-killing). Counts of GFP-positive cells in such wells stem from three pooled experiments.

(E) Counts of GFP-positive cells in individual wells following 24-hr co-culture with individual CTLs belonging to three pp65-specific CTL clones.

(F) Counts of GFP-positive cells in individual wells following 24-hr co-culture with individual CTLs expressing or not CD57 at their surface.

(G) Counts of GFP-positive cells in individual wells following 24-hr co-culture with individual CTLs from a primary clone and from four CTL sub-clones derived from wells in which a single CTL had eliminated all ten target cells.

See also Figures S2 and S3.

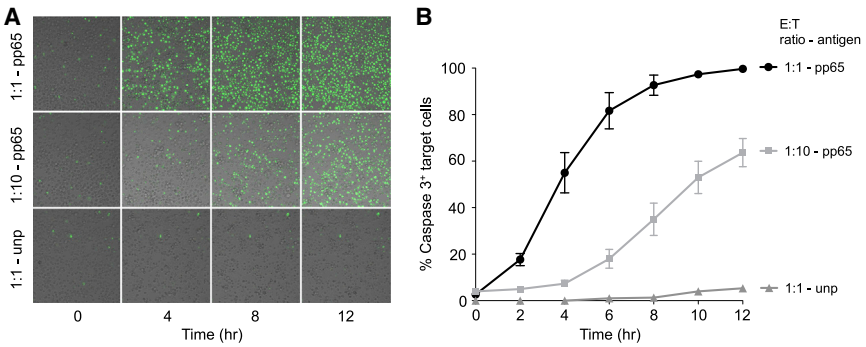

Figure 3. Distinct Killing Kinetics at High versus Low E:T Ratios

Target JY cells, pulsed with 100 nM pp65 or left unpulsed, were seeded at 100,000 cells in Lab-Tek chambers in the presence of CTLs at E:T ratios of 1:1 or 1:10. The NucView 488 caspase-3 substrate was used to track individual target cell killing by video-microscopy.

(A) Representative wide-field snapshots showing activation of caspase-3$^+$ at 0, 4, 8, and 12 hr after co-culture of target cells with CTLs in the indicated conditions.

(B) Quantification of videos as frequency of target cells activating caspase-3 over time. The mean ± SEM of three independent experiments is presented.

See also Movies S1, S2, and S3.

caspase-3 activation in target cells by time-lapse microscopy. Wide-field analysis at a 1:1 E:T ratio demonstrated a rapid cumulative rise in the proportion of target cells positive for active caspase-3, reaching a plateau corresponding to the nearly complete elimination of target cells within 6 hr (Figures 3A and 3B; Movies S1, S2, and S3). In contrast, at a 1:10 E:T ratio, a phase of latency was initially observed, during which caspase-3 activation was limited to a few target cells. Subsequent to this phase, a rise in caspase-3$^+$ target cells was observed, reaching 60% in 12 hr. This is in agreement with the very modest effect of the 1:10 E:T ratio in 4 hr observed in the bulk killing assay (Figure 1A) and reveals that at a low ratio, most killing events arise in a 6- to 12-hr window. To then assess the kinetics of CTL killing at a single-cell level, we seeded a 1:10 E:T ratio mixture onto a polydimethylsiloxane (PDMS) meshwork array of 100-μm-diameter microwells in a way to confine single CTLs and an excess of target cells in each microwell. Single-CTL killing kinetics confirmed the above-observed heterogeneity, since individual CTLs displayed a dispersed multiple killing performance ranging from 0 to 12 targets killed over 12 hr, with a mean of 4 target cells killed over 12 hr (Figures 4A and 4B; Movies S4, S5, and S6). The mean number of killed target cells was limited during the first 6 hr, while it progressively increased over the 6- to 12-hr time interval (Figure 4B). This single-CTL analysis therefore confirms that, in a context of an excess of target cells, the initial killing activity is relatively modest and is followed by an increased multiple killing activity in some CTLs.

We then aimed at characterizing the statistical nature of the heterogeneity of multiple killing observed in individual CTLs. Clearly, the killing time appears to follow an exponential law. As a consequence, the distribution of the killing time on the considered time window is a Poisson process whose unknown intensity is closely related to the parameter of the exponential law. With a dataset stemming from the analysis of 259 single CTLs in three independent experiments, we first evaluated with a chi-square test whether the cumulative number of killed target cells over 12 hr would distribute according to a single Poisson distribution (Supplemental Statistical Methods). Our analysis yielded a $T > 110$ (T is defined as a statistical quantity that indicates the goodness of fit of the null hypothesis to the data; see Supplemental Statistical Methods), leading to the rejection of this hypothesis with a type I error ≤ 0.001. Instead, the application of an expectation maximization algorithm indicated that the distribution of the 12-hr killing performance by the individual CTLs could be modeled by a mixture of two subsets (Figure 4C). Indeed, our data best fit with a mixed Poisson distribution composed by 66% of CTL killing in an average of 2.8 target cells and 34% of CTL killing in an average of 6.4 target cells. Our analysis yielded a $T < 8.9$, leading to the acceptance of the statistical assumption of a mixture of two Poisson distributions. Comparable results were obtained when considering the three data subsets separately (see Supplemental Statistical Methods). Our statistical analysis therefore implies that the intraclonal heterogeneity in multiple killing can be explained, at least in part, by a split of the clonal population into high-rate and low-rate killer CTL subsets.

To further investigate how the heterogeneity of individual CTL killing performance is shaped over time, we developed and applied a breakpoint test aimed at identifying the time at which the two CTL subsets diverge. Our statistical testing procedure is inspired by previous work on the detection of change in the mean for stationary Gaussian processes (GPs) based on the record method (Rychlik, 1990). We adapted this method to the case of a Poisson processes (PPs) by first computing the empirical mean of the killing among the population of CTLs to convert the observed PP to an approximately stationary GP according to the central limit theorem. Then, we used the test of Azais and Genz (Azais and Genz, 2013) to detect changes in the mean by taking into account the correlation structure learned in the time series (see Supplemental Information for a detailed description). Our breakpoint test indicates that the baseline hypothesis, namely that homogeneity in the mean is maintained all along the killing process, is rejected when considering the compiled dataset. The analysis indicates a first type error test lower than $p_{value} = 5.7 \times 10^{-4}$ with a breakpoint in the homogeneity likely to occur at about 10 hr (Figure 4D). Comparable results were obtained when considering the three data subsets separately (see Supplemental Information).

The registration of the prolonged killing kinetics of individual CTLs facing an excess of target cells therefore confirms the high heterogeneity in the killing efficiency measured with the end-point assay. In-depth statistical analysis further suggests a functional dichotomy within the CTL clonal population. Our datasets can therefore be explained as follows: most CTLs initially

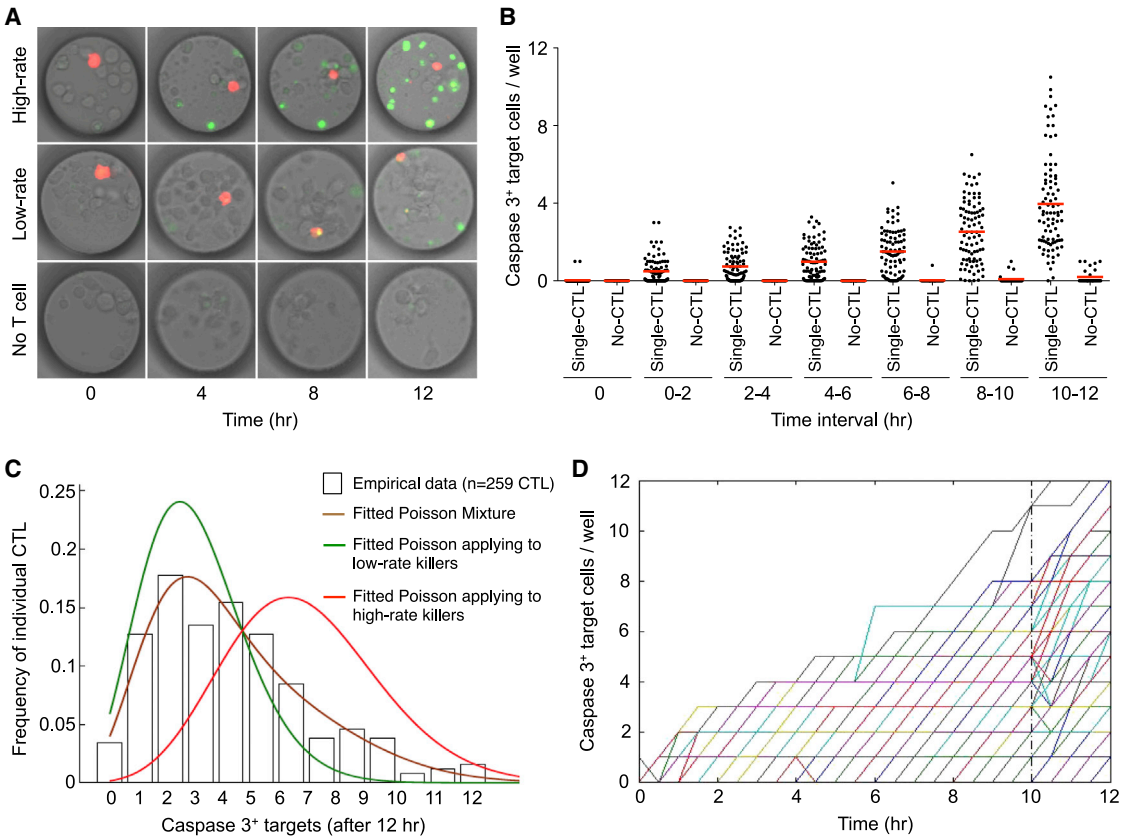

Figure 4. The Onset of High-Rate Killing Is Delayed and Restricted to a CTL Subset

Single calcein-stained CTLs were confined in 100-mm-diameter microwells and co-cultured with an excess of target JY cells for 12 hr in the presence of the NucView 488 caspase-3 substrate.

(A) Representative snapshots of microwells showing the CTL (in red) and the activation of caspase-3 in target cells (in green) at 0, 4, 8, and 12 hr in the indicated conditions.

(B) Quantification over the indicated time intervals of caspase-3$^+$ target cells from 88 microwells containing one CTL (gray dots) and 30 microwells without CTLs (brown dots). Data were pooled from three experiments. Bars indicate mean values.

(C) Frequency of individual CTLs according to the number of total caspase-3$^+$ target cells measured in 12 hr. Histograms represent empirical data (n = 259), while curves represent the single Poisson distributions applying to the low-rate and high-rate killer CTL subpopulations (green and red curves, respectively) or the complex Poisson distribution resulting from a mixture of the 2 single distributions and applying to the entire CTL population (brown curve).

(D) Killing kinetics of individual CTLs (n = 259, represented by different colors) measured as the number of caspase-3$^+$ target cells over 30-min time intervals. Although overlap does not allow visualization of each single CTL, the graph reveals accelerated killing pace in numerous CTLs after 10 hr (vertical dashed bar), which corresponds to the time at which the breakpoint analysis indicated the appearance of heterogeneity in the killing process.

See also Movies S4, S5, and S6.

behave as low-rate killer CTLs, while some of them develop as high-rate killer CTLs at later time points.

High-Rate Killing Relies on a Late Phase of Burst Killing Preceded by Isolated Killing Events

We then investigated which characteristics might distinguish the two subsets of CTLs. Based on the dataset comprising 259 single-CTL killing kinetics, we noticed that for most CTLs, the killing pace was highly irregular over the 12-hr period. In particular, some CTLs appeared to kill multiple target cells in a row with a burst kinetic (Figure 5A). To appreciate the killing pace of each CTL, we quantified the maximum killing rate reached during the 12-hr recording (considering a series of three consecutive killing events). Most CTLs killed with an irregular pace, as indicated by the fact that we detected killing-rate peaks above the theoretical average killing rate (Figure 5B). The maximum killing rates increased as a function of individual 12-hr killing performance to reach two to four killing events/hr in the CTLs managing to kill 9–12 targets cells over 12 hr. On the basis of this analysis, we defined burst killing as a serial killing of at least three targets at a rate of more than one target/hr, which is superior to the average killing rate of the best-performing CTLs (12 targets killed in 12 hr). The analysis of the compiled dataset revealed that 42% of the CTLs exhibited a burst killing phenotype. This CTL subset killed an average of 6.3 target cells over the 12-hr period. Furthermore, the distribution of the 12-hr killing performance according to the occurrence of burst killing revealed two subsets of CTLs that fitted the mixed Poisson

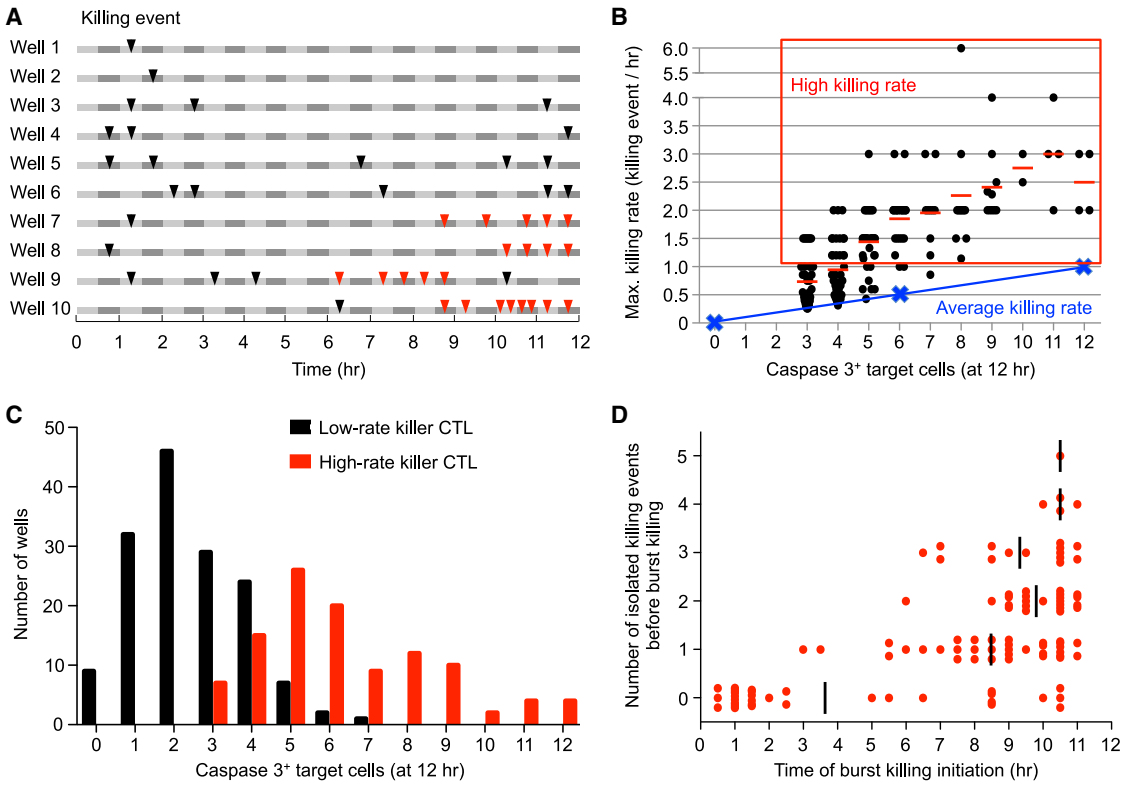

Figure 5. Burst Killing Is Preceded by Isolated Killing Events

(A) Schematic representation of killing events along the 12-hr observation interval in representative CTLs exposed to an excess of target cells in microwells. Black arrows represent isolated killing events, while red arrows represent burst killing events.

(B) Quantification of the maximum killing rate reached by each CTL during the 12-hr recording, considering a series of three consecutive killing events. The maximum killing rate of individual CTLs is plotted as a function of the 12-hr killing performance (number of targets cells killed after 12 hr). Bars represent mean values. The blue line indicates the theoretical average killing rate expected from CTLs that would kill at a regular pace.

(C) Frequency of individual CTLs (n = 259) divided into basic killers (black, rate of one cell/hr or no target cells/hr) and burst killers (red, rate more than one target cell/hr) according to the number of total caspase-3$^+$ target cells measured in 12 hr.

(D) Distribution of the burst killer CTLs according to both the number of isolated killing events (rate one cell/hr or no target cells/hr) preceding burst killing and the time of burst killing initiation. Bars indicate mean values.

distribution identified by our statistical analysis (Figure 5C). Together, these data indicate that a hallmark of high-rate killer cells is their capacity to accelerate killing pace to kill multiple target cells over a limited amount of time. We then investigated when these events of burst killing occurred. Interestingly, a majority of the burst killing events were initiated in an 8- to 11-hr time window (Figure 5D), which fits with the results from the breakpoint test. Our analysis further shows that in most cases, these events were preceded by one to three isolated killing events.

We then reasoned that the delayed onset of the burst killing might result from differences in killing initiation. The time delay before the first killing event occurred was indeed widely distributed among individual CTLs (Figure 6A). Actually, the proportion of CTLs killing at least one target cell was 59.1% in the initial 4-hr time window, while it increased to 96.5% over the 12-hr time window. This clearly indicates that the proportion of individual CTLs actively contributing to killing increased over time. When the CTL killing records were synchronized on the basis of the first killing event, a wide distribution in killing efficiency was observed after 4 or 6 hr (Figure 6B). This indicates that individual CTL killing heterogeneity cannot be explained by asynchrony in killing initiation. The synchronization of the killing records on the basis of the first killing event resulted in an anticipation of high-rate killing, as measured by the proportion of CTLs that displayed a burst killing activity (Figure 6C). This is in agreement with the above observation that burst killing events were preceded by isolated killing events. Interestingly, the synchronization abolished the lag phase, which was replaced by a progressive increase in the proportion of high-rate killer CTLs. These data show that the subset of high-rate killer CTLs is characterized by a burst killing process, which develops progressively over a period of 10 hr following the first killing event. The global killing activity of a clonal CTL population at a low E:T ratio is therefore a cumulative process relying on the progressive recruitment of actively killing CTLs over time and on the onset of a delayed high-rate killing activity in a fraction of the CTLs.

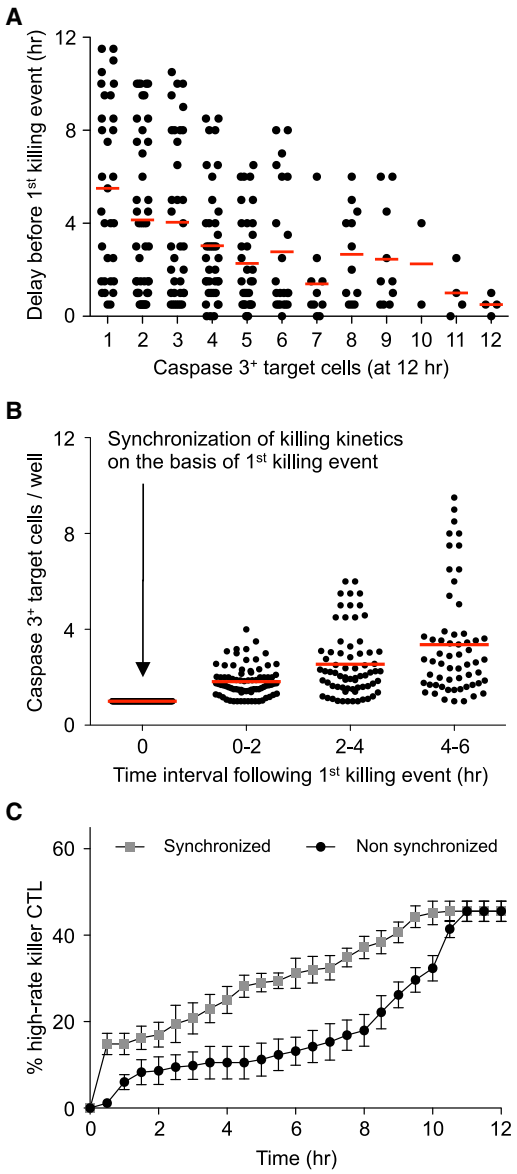

Figure 6. Variability of Delays in Killing Initiation Does Not Account for Heterogeneous Burst Killing

(A) Time delay before the first killing event analyzed for each CTL (n = 259) as a function of its 1-hr killing performance. Data represent mean values.

(B) Kinetics of multiple killing events following the first killing event is represented after alignment of the killing records so that time 0 corresponds in each well to the appearance of the first caspase-3$^+$ target cell.

(C) Cumulative frequency of CTL displaying burst killing, with or without synchronization of the killing kinetics on the basis of the first killing event. Data represent mean ± SEM from three experiments.

CTL Activation Requirements for the Onset of High-Rate Killing

The delay in the onset of high-rate killing might be related to the requirement of a TCR-driven activation process upon interaction of the CTL with the first target cells it encounters. We and others have shown that CTL-mediated killing can be triggered at a very low TCR stimulation threshold that does not lead to full activation (Huppa et al., 2003; Sykulev et al., 1996; Valitutti et al., 1996). We therefore asked whether picomolar concentrations of peptide sufficient to trigger early killing would be able to efficiently sustain killing over prolonged time frames. CTL stimulated with 10 pM failed completely to produce interferon-γ (IFN-γ) while partially maintaining the capacity to secrete perforin (Figure 7A). However, this low peptide concentration was sufficient to trigger a robust killing in 4 hr at a 2:1 E:T ratio (Figure S4). In contrast, this only led to a very limited sustainment of killing over 12 hr (Figure 7B). In agreement, the proportion of CTLs displaying a burst killing was drastically reduced (Figure 7C). To further assess the CTL activation requirements for the onset of the secondary phase of high-rate killing, CTL clones were cocultured with an excess of target cells in the presence of cyclosporin A (CsA) as a means to reduce CTL effector functions. As expected, CsA treatment strongly impaired the neo-synthesis of IFN-γ, while it did not affect the secretion of prestored perforin in CTLs stimulated for 4 hr by pulsed target cells (Figure 7A). Accordingly, CsA treatment did not interfere significantly with early killing potential, as measured after 4 hr at a 2:1 E:T ratio (Figure S4). However, CsA treatment reduced significantly the onset of the late-developing high-rate killing (Figures 7D and 7E). Together, these data show that the onset of high-rate killing is affected by suboptimal T cell stimulation.

DISCUSSION

By assessing prolonged killing kinetics of human CTL clones at a single-cell level in conditions of target cell excess, we reveal the ability of individual CTLs to perform multiple killing in a sustained manner. Remarkably, individual CTLs displayed highly heterogeneous multiple killing activity. This heterogeneity was mainly due to the delayed development of a burst killing activity, which was restricted to approximately one-third of the CTL population. Our study therefore reveals an aspect of CTL killing activity, whereby the basal killing activity shared among individual CTLs is followed by the emergence of a split behavior characterized by the initiation of burst killing activity in a subset of CTLs. Such heterogeneity, however, does not correspond to an inheritable specialization, since it is reset in the progeny of individual CTLs. The observed heterogeneity in the ability of individual CTLs to control an excess of target cells appeared to be mainly T cell intrinsic for the following reasons. First, killing heterogeneity was observed independently from the location of the CTL relative to the target cells. Second, a comparable level of heterogeneity was measured using wells of distinct geometry and confinement. Third, the micromesh experiments were not consecutive to a cell-sorting approach, therefore excluding the possibility that such procedure would affect CTL viability. Fourth, we considered for our analysis only wells in which the CTLs remained positive for calcein, thereby implying that the CTLs analyzed were still alive at the end of the experiments.

We show here that the sensitivity of CTL-mediated killing can be best appreciated by measuring, over prolonged time frames, the impact of limited CTL numbers on the survival of an excess of target cells. In our model of human CTL clones recognizing a CMV peptide presented by EBV-transformed B cells, a

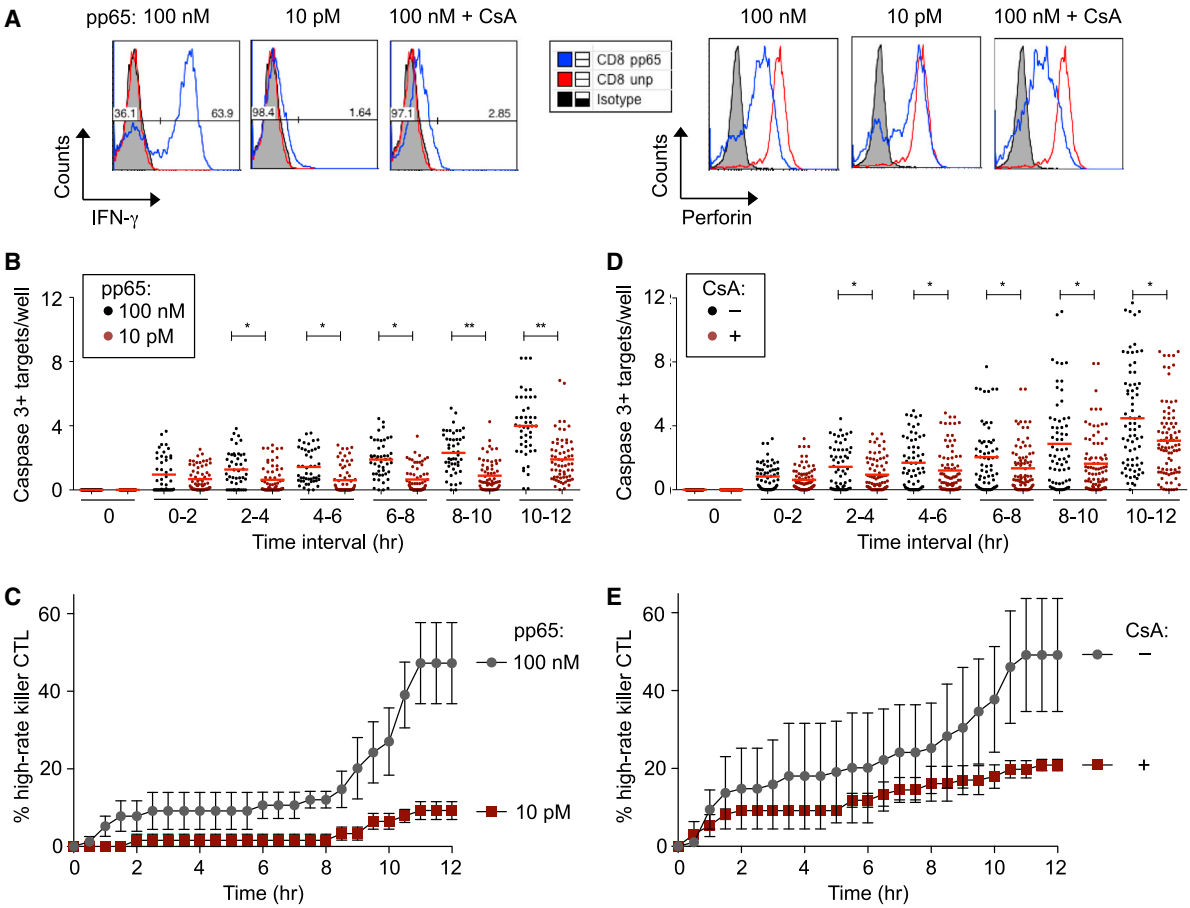

Figure 7. Strong CTL Activation Required for the Onset of High-Rate Killing

(A) Histogram plots representing the production of IFN-γ and the release of perforin by CTLs co-cultured with a 10-fold excess of target JY cells pulsed with 100 nM or 10 pM pp65, in the presence or absence of CsA.

(B) Quantification over the indicated time intervals of caspase-3$^+$ target cells from 61 microwells with one CTL and target cells pulsed with 100 nM pp65 (gray dots) and 64 microwells with one CTL and target cells pulsed with 10 pM pp65 (brown dots). Data were pooled from three experiments. Bars indicate mean values. p values are results of t tests between indicated conditions (*$p < 0.05$; **$p < 0.001$).

(C) The effect of pp65 concentration on the occurrence of high-rate killer CTLs, as represented by the frequency of CTLs displaying burst killing. Data represent mean ± SEM from three experiments.

(D) Quantification over the indicated time intervals of caspase-3$^+$ target cells from 56 microwells with one CTL and untreated pulsed target cells (gray dots) and 70 microwells with one CTL and CsA-treated pulsed target (brown dots). Data were pooled from three experiments. Bars indicate mean values. p values are results of t tests between indicated conditions (*$p < 0.05$; **$p < 0.001$).

(E) The effect of CsA treatment on the occurrence of high-rate killer CTLs, as represented by the frequency of CTLs displaying burst killing. Data represent mean ± SEM from three experiments.

See also Figure S4.

reproducible impact on the target cell population was measured at an E:T ratio as low as 1:40. Importantly, near-complete elimination of the target cell population was obtained with a 1:10 E:T ratio. Such a level of killing has not been reported previously for human CTLs. By revealing a previously undetected CTL killing efficiency, our assays might be more sensitive than classical 4-hr killing assays in predicting CTL efficiency in the context of CTL-based therapies. As compared to in vivo settings, our approaches, however, fail to reproduce the 3D environment encountered in tissues. Nevertheless, our data are comparable to those obtained with murine CTLs embedded in 3D collagen matrix (Weigelin and Friedl, 2010). This indicates that the multiple killing activity measured here is intrinsic to CTLs and that the 3D matrix environment encountered in tissues should not fundamentally modify this property.

Beyond testing the limits of CTL killing efficiency, our study provides kinetic measurements of multiple killing events over time, both at the population and single-cell levels. Clearly, our data show that the killing activity of human CTL clones is a cumulative process, which results from a non-synchronized and non-linear accumulation of killing events. Following an initial phase of latency during which a relatively low number of target cells activated caspase-3, an accumulation of killing events was measured. Comparable kinetics were observed under bulk and

single-CTL settings, implying that they did not result from the initiation of synergistic cooperation among CTLs. We show that the delayed onset of an increased killing activity is preceded by isolated events of low-pace killing. Strikingly, similar burst kinetics have been recently described for natural killer (NK) cell killing activity, using a reporter of granzyme B activity in target cells (Choi and Mitchison, 2013). Together, these data suggest that upon a first kill, both CTLs and NK cells get primed for quicker successive kills. Such behavior might be facilitated by the high target cell density used in both models, allowing killer cells, once they have established multiple contacts, to kill neighbor targets cells at increased frequency.

Our work extends the recent findings on NK cells, since it demonstrates that functional heterogeneity applies to genetically identical clonal populations, which could not be defined in the NK cell models. Moreover, our statistical analysis suggests the emergence of a functional dichotomy in the killing behavior of CTLs belonging to a clonal population. The identification of high-rate killer CTLs is in agreement with our previous demonstration that CTLs can kill multiple target cells encountered simultaneously (Wiedemann et al., 2006). In vivo imaging has shown that CTLs and NK cells use distinct killing strategies, since, as compared to NK cells, CTL engage in more stable contacts with their target cells (Deguine et al., 2010). It will therefore be interesting to extend our observations to in vivo settings to measure the kinetics of multiple killing in killer cells using live microscopy.

Our study shows that a single CTL can kill up to 12 target cells sequentially within a time frame of 12 hr. The onset of such high-rate killing is dependent on efficient CTL activation via TCR engagement as revealed by the reduction of high-rate killing at low peptide concentrations and following CsA treatment. Our data clearly indicate that the killing activity of a single CTL is sustained over 12 to 24 hr. Although we did not measure multiple killing by individual CTLs beyond 24 hr, we cannot exclude that CTLs could keep killing beyond this time frame. However, the fact that, after 24 hr, residual target cells progressively escape the control exerted by CTLs strongly suggests that CTLs globally lose cytotoxic potential. Whether this is due to progressive exhaustion, limited refilling of lytic potential, or death will need to be addressed in further studies.

A major finding of this work is that genetically and phenotypically homogeneous CTL clonal populations are composed of individual CTLs harboring a wide range in ability to perform multiple killing over extended time frames. In a previous study, the isolation of primary $CD8^+$ T cells specific for a HIV GAG epitope in single-cell arrays has shown that only a minority of CTLs could concomitantly kill and secrete IFN-γ (Varadarajan et al., 2011). Although highlighting the fact that not all effector CTLs might be equally efficient at killing target cells, this study assessed neither multiple killing over prolonged time periods nor the spread of individual CTL killing performance. Furthermore, the functional diversification reported might be linked to the polyclonal nature of the $CD8^+$ T cells studied, since in our clonal model, most CTL were able to both kill and produce IFN-γ.

Importantly, the individual heterogeneity in cytotoxic activity parallels that recently described for expansion rate and differentiation of $CD8^+$ T cell precursors (Buchholz et al., 2013; Gerlach et al., 2013). Collectively, these data reveal that the key steps of CTL responses are established on the basis of a high variability of individual behaviors. Strikingly, individual heterogeneity in both expansion and killing results in a very constant output at the population level. Therefore, individual heterogeneity might have evolved as a way to guarantee reproducible CTL responses via an averaging process. The heterogeneity reported here appears to be intrinsic to the phenomenon of multiple killing.

A puzzling question is how the described distribution in killing performance of individual CTLs is produced. It is possible that individual differences in CTL motility and scanning will condition the ability to establish productive contacts with multiple target cells. However, such differences might be difficult to pick, since we observed that most CTLs within the microwells establish rosette-like cellular complexes with the target cells, independently of their multiple killing performance. The ability to develop as high-rate killer CTLs might depend on an activation threshold that is reached only for a fraction of the population. The described heterogeneity might also result from differences in the state or number of key molecules controlling the TCR-driven release of lytic molecules. Computational modeling has shown that phenotypic variability can be achieved in a controlled manner by regulated variation in the expression of a few key signaling molecules such as CD8, ERK, and SHP-1 (Feinerman et al., 2008). On the other hand, analysis of multiple genes at a single-cell level has highlighted how the coexpression of different effector genes in $CD8^+$ T cells is associated to the functional activity of the corresponding cells (Peixoto et al., 2007). Our subcloning experiment indicates that $CD8^+$ T cells reset functional heterogeneity following a few cycles of interaction with target cells. These individual cells do not appear to retain their specific properties in their progeny, excluding the possibility that such differences would be epigenetically imprinted. Maintaining heterogeneity therefore appears a key principle in CTL to guarantee that any given antigen-specific population will generate reproducible outcomes in terms of expansion dynamics, killing efficiency, and differentiation.

What is the advantage for the non-genetic inter-individual variability observed here for cytotoxic function? Our data and analysis support the following model: an initial low-rate killing activity is shared among most individuals. This may be sufficient to eliminate a sensitive target cell population at high E:T ratios. If target cells persist after the initial phase of cytotoxicity (low E:T ratio, or resistant target cells), the process of high-rate killing is launched in some of the CTLs. Therefore, the sustained cytotoxicity mediated by a CTL population is a non-linear cumulative process. It is tempting to speculate that such a gradual process might allow the calibration of CTL responses, allowing adaptation of the whole CTL population to the resistance of the opposing target cell population or to the persistence of the antigenic stimulus. The scalability of cytokine production by $CD4^+$ T cell populations has recently been shown to depend on the proportion of individual T cells engaging digitally into cytokine output (Huang et al., 2013). Our study indicates that the regulation of the CTL response obeys a distinct rule. Indeed, the scalability of killing appears to depend on the proportion of individual T cells engaging into an increased lytic potential if required by the excess of target cells.

In conclusion, our study unravels a previously unappreciated level of functional heterogeneity in individual cells belonging to clonal populations of effector CTLs. Such heterogeneity appears to set the performance of CTLs to control an excess of target cells at the population level. We reveal that the prolonged CTL activity relies on a dual strategy combining low-rate killing by a majority of cells and delayed onset of high-rate killing by a limited proportion of cells. In the context of CTL-based approaches, our findings on the intraclonal heterogeneity of the killing rate of individual CTLs call for a re-evaluation of the precise performance of CTLs and identify individual heterogeneity as a key parameter in evaluating CTL performance in health and disease.

EXPERIMENTAL PROCEDURES

Human CD8$^+$ T Cell Lines and Clones

Peripheral blood mononuclear cells (PBMCs) were isolated from buffy coats of healthy donors obtained through the Etablissement Français du Sang (EFS Midi-Pyrénées, Purpan University Hospital, Toulouse, France). Blood samples were collected and processed following standard ethical procedures (Helsinki protocol), after obtaining written informed consent from each donor and approval for this study by the local ethics committee (Comité de Protection des Personnes Sud-Ouest et Outremer II). Human CD8$^+$ T cell lines were purified from healthy donor blood samples using the RosetteSep Human CD8$^+$ T Cell Enrichment Cocktail (STEMCELL Technologies). Cells were seeded at 5 × 10^5 cells/ml in complete medium consisting of RPMI 1640 supplemented with 8% human AB serum (PAA), minimum essential amino acids, HEPES, and sodium pyruvate (Invitrogen). For cloning, single HLA-A2-restricted CD8$^+$ T cells specific for the NLVPMVATV peptide of the CMV pp65 protein were distributed in 96-well U-bottom plates using a BD FACSAria II cell sorter operating in "single-cell purity" sorting mode. CD8$^+$ T cells were stimulated in the presence of 1 × 10^6/ml irradiated allogeneic PBMCs and 1 × 10^5/ml irradiated EBV-transformed JY cells and 2 μg/ml phytohemagglutinin in the case of CD8$^+$ T cell clones or SAg mixture (100 ng/ml staphylococcal enterotoxin B, staphylococcal enterotoxins A, staphylococcal enterotoxin E, and toxic shock syndrome toxin-1 from Toxin Technology) in the case of CD8$^+$ T cell lines. CD8$^+$ T cells were supplied with 100 IU/ml human rIL-2 was added on day 3 and restimulated every 2 weeks.

Residual Live Target Cell Quantification

HLA-A2-matched EBV-transformed B cells (JY) were used as target cells and pulsed with pp65 (at 10 pM or 100 nM) when cocultured with CTL clones or 1 ng/ml of SAg mixture when cocultured with CD8$^+$ T cell lines. For cytotoxic assays, target cells were left unpulsed or pulsed during 2 hr at 37°C/5% CO_2, washed three times, and subsequently transferred to a 96 well plate U-bottom at 1 × 10^5 cells/100 μl complete medium without interleukin-2 (IL-2). CD8$^+$ T cells prestained with 0.1 μM of CellTracker Green CMFDA (5-chloromethylfluorescein diacetate from Invitrogen) for 20 min at 37°C/5% CO_2 were added to the target cells at indicated ratios in 100 μl complete medium without IL-2. Cells were pelleted for 1 min at 1,500 rpm and incubated at 37°C/5% CO_2 from 4 to 72 hr. In some experiments, 10 μg/ml anti-FasL antibodies (clone NOK-1; BD Pharmingen) or 0.05 μg/ml aphidicolin (Sigma) treatment was performed during 24-hr assays. A 50-μl solution made of PBS containing 10% 7-AAD (BD Pharmingen) and 5% BD CompBead (BD Pharmingen) was added 10 min before flow cytometry analysis to measure the percentage of lysed target cells or estimate the number of residual live cells. A reference tube consisting of 1 × 10^5 JY cells in 200 μl plus 50-μl bead solution was acquired until reaching 2,000 beads. In the experimental tubes, acquisition was also fixed to 2,000 beads. The absolute number of residual live target cells was calculated by multiplying the number of events collected in the CFMDA$^-$/7-AAD$^-$ gate by the ratio set by the reference tube. All data were acquired on a BD FACSCalibur cytometer and analyzed using FlowJo software.

Fluorescence-Activated Cell Sorter-Assisted Clonal Killing Assay

Ten GFP-expressing target cells either unpulsed or pulsed with 100 nM pp65 were distributed in 96-well U-bottom low-cell-binding plates (Nunc Dishes) using a BD FACSAria II cell sorter operating in single-cell-purity sorting mode. Sequentially, 1 or 20 CD8$^+$ T cell clones prestained with 0.5 μM CellTrace calcein red-orange (Invitrogen) for 30 min at 37°C/5% CO_2 were distributed in the same microplate wells followed by 5-min centrifugation at 1,500 rpm. After 24-hr incubation at 37°C/5% CO_2, every well was then examined using an Apotome Axio-observer confocal microscope (Zeiss) with a 10× Plan-Neofluar objective for residual GFP-expressing JY cell enumeration.

Confocal Video-Microscopy for Real-Time Caspase-3 Activation

For live cell imaging, 1 × 10^5 pulsed target cells were seeded into microchambers (Lab-Tek Chambered coverglass; Nalgen Nunc) previously coated with poly-D lysine (Sigma), followed by addition of 2 μM NucView 488 caspase-3 substrate (Biotium) and CD8$^+$ T cell clones prestained with 0.5 μM CellTrace calcein red-orange (Invitrogen) in different ratios at the beginning of the recording. Where indicated, a confined single CD8$^+$ T cell clone multiple killing evaluation was performed in microchambers pre-coated with PDMS micromesh arrays (Microsurfaces) containing 100-μm-diameter wells. In some experiments, 1 μg/ml CsA or 10pM pp65 pulsing was performed in parallel. Every 2 min, one image was acquired during 12 hr using either a LSM 510 or a 710 confocal microscope (Zeiss) with a 20× Plan Apo objective equipped with an environmental chamber kept at 37°C and 5% CO_2 and the pinhole was opened to 10 μm to capture maximum fluorescence.

Measurement of IFN-γ and Perforin Loss

Target cells were either unpulsed or pulsed with 100 nM pp65 were cocultivated with CD8$^+$ T cell clones prestained with 0.1 μM CellTracker Green CMFDA (5-chloromethylfluorescein diacetate from Invitrogen) at 1:10 E:T ratio during 4 hr. In some experiments, 10 μg/ml brefeldin A (Sigma) and/or 1 μg/ml CsA was added to the culture. Cells were fixed with 2% paraformaldehyde, permeabilized with 0.1% saponin (in PBS/3% BSA/HEPES), stained with AF700-labeled anti-IFN-γ monoclonal antibody (clone XMG1.2; BD Biosciences), and AF647-labeled anti-human perforin monocolonal antibody (clone δG9; BioLegend). Data were acquired on a BD LSR Fortessa cytometer and analyzed using FlowJo software.

Image Data Analyses

For image analysis, the freeware ImageJ v1.47b and the LOCI plug-in were downloaded from the National Institutes of Health websites (http://rsb.info.nih.gov/ij and http://loci.wisc.edu/software/bio-formats, respectively). To perform automated counting of caspase-3$^+$ cells through time, images were binarized and further processed using the erosion, dilatation, and watershed ImageJ tools. For the single-CTL assay, microwells were selected on the basis of the presence of a single calcein-stained CTL all along the 12-hr movie by visual inspection. Killing scores were measured as mean of caspase-3$^+$ cells over 2-hr time intervals.

SUPPLEMENTAL INFORMATION

Supplemental Information includes Supplemental Statistical Methods, four figures, and six movies and can be found with this article online at http://dx.doi.org/10.1016/j.celrep.2015.05.002.

AUTHOR CONTRIBUTIONS

Z.V. performed the experiments, analyzed the results, and wrote the paper; S.M. and W.Y. generated the CTL clones; C.C. and S.G. performed the statistical analysis; D.G. analyzed the single-CTL video-microscopy data; S.V. designed the research and wrote the paper; and L.D. designed the research, supervised the experiment analysis, and wrote the paper.

ACKNOWLEDGMENTS

We wish to thank Fatima-Ezzahra L'Faqihi-Olive, Valérie Duplan-Eche, Delphine Lestrade, and Manon Farcé from the CPTP cytometry platform, as

well as Sophie Allart and Astrid Canivet from the CPTP microscopy platform. We are grateful to Eric Espinosa for helpful discussion and suggestions. We thank Nicolas Fazilleau and Corine Perals for CTL clone characterization and discussion. We also thank Daniel Dunia for discussion. This work was supported by the Brazilian post-doctoral programs from CAPES (6486/10-0) and CNPq (237654/2012-1). Z.V. is supported by PAPES V and FAPERJ. W.Y. received funding support from the Damon Runyon Cancer Research Foundation (postdoctoral fellowship) and the NIH (grant 1K08DK093709-01). This work also benefited from funding from the Fondation ARC pour la Recherche sur le Cancer (grants EML2012090493 and SL220100601347), the Institut National du Cancer (Grant INCa 2012-054), and the Agence Nationale de la Recherche (Laboratoire d'Excellence Toulouse Cancer). The funders had no role in study design, data collection and analysis, decision to publish, or preparation of the manuscript.

Received: January 12, 2014
Revised: February 16, 2015
Accepted: May 1, 2015
Published: May 28, 2015

REFERENCES

Azais, J.M., and Genz, A. (2013). Computation of the distribution of the maximum of stationary Gaussian processes. Methodol. Comput. Appl. Probab. *15*, 969–985.

Beuneu, H., Lemaître, F., Deguine, J., Moreau, H.D., Bouvier, I., Garcia, Z., Albert, M.L., and Bousso, P. (2010). Visualizing the functional diversification of CD8+ T cell responses in lymph nodes. Immunity *33*, 412–423.

Buchholz, V.R., Flossdorf, M., Hensel, I., Kretschmer, L., Weissbrich, B., Gräf, P., Verschoor, A., Schiemann, M., Höfer, T., and Busch, D.H. (2013). Disparate individual fates compose robust CD8+ T cell immunity. Science *340*, 630–635.

Choi, P.J., and Mitchison, T.J. (2013). Imaging burst kinetics and spatial coordination during serial killing by single natural killer cells. Proc. Natl. Acad. Sci. USA *110*, 6488–6493.

Deguine, J., Breart, B., Lemaître, F., Di Santo, J.P., and Bousso, P. (2010). Intravital imaging reveals distinct dynamics for natural killer and CD8(+) T cells during tumor regression. Immunity *33*, 632–644.

Dustin, M.L., and Long, E.O. (2010). Cytotoxic immunological synapses. Immunol. Rev. *235*, 24–34.

Faroudi, M., Utzny, C., Salio, M., Cerundolo, V., Guiraud, M., Müller, S., and Valitutti, S. (2003). Lytic versus stimulatory synapse in cytotoxic T lymphocyte/target cell interaction: manifestation of a dual activation threshold. Proc. Natl. Acad. Sci. USA *100*, 14145–14150.

Feinerman, O., Veiga, J., Dorfman, J.R., Germain, R.N., and Altan-Bonnet, G. (2008). Variability and robustness in T cell activation from regulated heterogeneity in protein levels. Science *321*, 1081–1084.

Gerlach, C., Rohr, J.C., Perié, L., van Rooij, N., van Heijst, J.W.J., Velds, A., Urbanus, J., Naik, S.H., Jacobs, H., Beltman, J.B., et al. (2013). Heterogeneous differentiation patterns of individual CD8+ T cells. Science *340*, 635–639.

Huang, J., Brameshuber, M., Zeng, X., Xie, J., Li, Q.-J., Chien, Y.-H., Valitutti, S., and Davis, M.M. (2013). A single peptide-major histocompatibility complex ligand triggers digital cytokine secretion in CD4(+) T cells. Immunity *39*, 846–857.

Huppa, J.B., Gleimer, M., Sumen, C., and Davis, M.M. (2003). Continuous T cell receptor signaling required for synapse maintenance and full effector potential. Nat. Immunol. *4*, 749–755.

Lemaître, F., Moreau, H.D., Vedele, L., and Bousso, P. (2013). Phenotypic CD8+ T cell diversification occurs before, during, and after the first T cell division. J. Immunol. *191*, 1578–1585.

Macken, C.A., and Perelson, A.S. (1984). A multistage model for the action of cytotoxic T lymphocytes in multicellular conjugates. J. Immunol. *132*, 1614–1624.

Peixoto, A., Evaristo, C., Munitic, I., Monteiro, M., Charbit, A., Rocha, B., and Veiga-Fernandes, H. (2007). CD8 single-cell gene coexpression reveals three different effector types present at distinct phases of the immune response. J. Exp. Med. *204*, 1193–1205.

Perelson, A.S., and Bell, G.I. (1982). Delivery of lethal hits by cytotoxic T lymphocytes in multicellular conjugates occurs sequentially but at random times. J. Immunol. *129*, 2796–2801.

Poenie, M., Tsien, R.Y., and Schmitt-Verhulst, A.M. (1987). Sequential activation and lethal hit measured by [Ca2+]i in individual cytolytic T cells and targets. EMBO J. *6*, 2223–2232.

Purbhoo, M.A., Irvine, D.J., Huppa, J.B., and Davis, M.M. (2004). T cell killing does not require the formation of a stable mature immunological synapse. Nat. Immunol. *5*, 524–530.

Rothstein, T.L., Mage, M., Jones, G., and McHugh, L.L. (1978). Cytotoxic T lymphocyte sequential killing of immobilized allogeneic tumor target cells measured by time-lapse microcinematography. J. Immunol. *121*, 1652–1656.

Rychlik, I. (1990). New bounds for the first passage, wavelength and amplitude density. Stochastic Process. Appl. *34*, 313–339.

Sykulev, Y., Joo, M., Vturina, I., Tsomides, T.J., and Eisen, H.N. (1996). Evidence that a single peptide-MHC complex on a target cell can elicit a cytolytic T cell response. Immunity *4*, 565–571.

Thorn, R.M., and Henney, C.S. (1976). Kinetic analysis of target cell destruction by effector T cells. I. Delineation of parameters related to the frequency and lytic efficiency of killer cells. J. Immunol. *117*, 2213–2219.

Valitutti, S., Müller, S., Dessing, M., and Lanzavecchia, A. (1996). Different responses are elicited in cytotoxic T lymphocytes by different levels of T cell receptor occupancy. J. Exp. Med. *183*, 1917–1921.

Varadarajan, N., Julg, B., Yamanaka, Y.J., Chen, H., Ogunniyi, A.O., McAndrew, E., Porter, L.C., Piechocka-Trocha, A., Hill, B.J., Douek, D.C., et al. (2011). A high-throughput single-cell analysis of human $CD8^+$ T cell functions reveals discordance for cytokine secretion and cytolysis. J. Clin. Invest. *121*, 4322–4331.

Weigelin, B., and Friedl, P. (2010). A three-dimensional organotypic assay to measure target cell killing by cytotoxic T lymphocytes. Biochem. Pharmacol. *80*, 2087–2091.

Wiedemann, A., Depoil, D., Faroudi, M., and Valitutti, S. (2006). Cytotoxic T lymphocytes kill multiple targets simultaneously via spatiotemporal uncoupling of lytic and stimulatory synapses. Proc. Natl. Acad. Sci. USA *103*, 10985–10990.

Zeijlemaker, W.P., van Oers, R.H., de Goede, R.E., and Schellekens, P.T. (1977). Cytotoxic activity of human lymphocytes: quanitative analysis of T cell and K cell cytotoxicity, revealing enzyme-like kinetics. J. Immunol. *119*, 1507–1514.

Cell Reports

Supplemental Information

Individual Human Cytotoxic T Lymphocytes Exhibit Intraclonal Heterogeneity during Sustained Killing

Zilton Vasconcelos, Sabina Müller, Delphine Guipouy, Yu Wong, Claire Christophe, Sébastien Gadat, Salvatore Valitutti, and Loïc Dupré

Statistical analysis of the distribution of individual CTL killing efficacy, Related to Figure 4

On the basis of the data obtained from the single-CTL killing assay, we assumed that each CTL (referred as c) has an individual ability of killing, which is distributed according to a time-inhomogeneous *Poisson Process*, whose intensity $(\lambda_c(t))_{t>0}$ is unknown. The experimental data indicate that $\lambda_c(t)$ increases with t, from the initialization 0 to the ending time Te =12 hrs.

We were primarily interested in evaluating the homogeneity of the whole population of CTL with respect to the intensity λ_c. In order to assess this homogeneity, a statistical study was conducted. For each of the n CTL analyzed (n=259), we recorded the cumulative number of killed target cells during the first Te hr after the initialization of the killing process. From the *Poisson Process* homogeneity assumption, the same intensity λ is commonly shared by each CTL and the cumulative number N_c of killed target cells is distributed according to a *Poisson Distribution* whose parameter Λ corresponds to the integral of $\lambda(t)$ between 0 and Te:

$$\Lambda = \int_0^{Te} \lambda(t)\, dt.$$

Hence, even though Λ is still unknown, we can test the homogeneity of the observations N_c when c varies: $0 < c < 260$. In this view, we applied a Chi-square test to the *Poisson Distribution*, whose parameter is the observed average value of the cumulative numbers of killed target cells :

$$S= n^{-1} (N_1 + N_2+...+N_n).$$

Remark that an average value S of 4.06 was obtained. The Chi-Square statistics is :

$$T = n \Sigma_{0 \le k \le 12} (p_e(k)-p_S(k))^2/p_S(k),$$

where k varies from 0 to 12. The empirical frequency that one CTL killed k target cells is designed as $p_e(k)$, it is the number of observations such that $N_c = k$ divided by n. The theoretical *Poisson* frequency $p_S(k)$ is the given by :

$$p_S(k) = e^{(-S)}\ S^k/k! \text{ if } k<12 \text{ and } p_S(12) = e^{(-S)}\ [S^{12}/12!+S^{13}/13!+...].$$

The last theoretical frequency is the size of the *Poisson* upper tail after 12. We obtained that

the statistics T is greater than 113 in our numerical experiment. This statistics is much larger than the $1\text{-}10^{-8}$ quantile of the Chi-Square distribution of 13-2 = 11 degrees of freedom (which is the reference distribution since we have to estimate the mean value of the *Poisson Distribution*). Hence, we reject the homogeneity assumption of the CTL population with a type I error lower than 10^{-8}.

We then reasoned that the collected data might fit *a mixture of two Poisson Distributions.*

Using an *Expectation Maximization algorithm (EM algorithm)*, the estimator of mixture parameter is :

$$\theta^*=(0.66,0.34,2.8,6.4).$$

This means that the CTL population is divided in two subpopulations : 66% of the CTL follow a *Poisson Distribution* with an average of 2.8 killed target cells over 12 hr, while 34% of the CTL follow a *Poisson Distribution* with an average of 6.4 killed target cells over 12 hr.

From a statistical point of view, the above formula may now be replaced by :

$$T' = n \sum_{0 \le k \le 12} (p_e(k)-p_{mix}(k))^2/p_{mix}(k),$$

where $p_{mix}(k)$ is the theoretical frequency obtained with the above *Poisson* mixture model.

$$p_{mix}(k) = q\, p_{6.6}(k)+(1-q)\, p_{3.3}(k).$$

T' is significantly reduced (T' = 8.9 in our experiment), which yields the acceptation of the statistical assumption of a *mixture of two Poisson Distributions* (the type I error would be of about 45%).

As the 259 observations come from 3 independent experiments, Chi-square tests were applied separately to each data subset.

- The Chi-square test of homogeneity of the 88 CTL killing (first subset) is associated to a type I error lower than = 0.003, leading to the rejection of the homogeneity assumption of the CTL population. In addition the Chi-square statistics of goodness-of-fit test of the observations to the *mixture distribution* is lower than 12.33, which yields the acceptation of the assumption of a *mixture distribution* (the type I error would be of

15%).

The estimator of mixture parameter obtained using *EM algorithm* is :

$\theta^*=(0.77,0.23,3.26,6.9)$.

- The Chi-square test of homogeneity of the 97 CTL killing (second subset) is associated to a type I error lower than = $8.9\ 10^{-4}$, leading to the rejection of the homogeneity assumption of the CTL population. In addition the Chi-square statistics of goodness-of-fit test of the observations to the *mixture distribution* is lower than 8.25, which yields the acceptation of the assumption of a *mixture distribution* (the type I error would be of 51%).

The estimator of mixture parameter obtained using *EM algorithm* is :

$\theta^*=(0.6,0.4,2.45,7.1)$.

- The Chi-square test of homogeneity of the 75 CTL killing (third subset) is associated to a type I error lower than = 0.066. This does not clearly lead to reject the homogeneity assumption of the CTL population of homogeneity of the CTL population. Noting that the Chi-square statistics of goodness-of-fit test of the observations to the *mixture distribution* is lower than 8, which yields to the type I error would be of 0.20, then we favor the hypothesis of *mixture distribution* for the observations.

The estimator of mixture parameter obtained using *EM algorithm* is :

$\theta^*=(0.97,0.03,3.5,4.84)$.

To the light of the estimator θ^*, as one distribution has a proportion very low (0.03), that call into question the *mixture distribution* of the observations.

Statistical analysis of cumulative killing kinetics, Related to Figure 4

We describe below the statistical test for the detection of a change in the mean of the counting process involved in the CTL activity. For any CTL i among the n available ones, we denote

$X_i(t)$ the number of target cells killed at time t. The time t varies in our experiment between 0 and 12 hr, sampled every 30 min (one unit below corresponds to half an hour). The averaged killing process is then :

$$m_X(t) = [X_1(t)+X_2(t)+...+X_n(t)] /n,\ t=\{1, 2, ... 24\} \text{ half an hours,}$$

and can be considered as an approximately GP thanks to the Central Limit Theorem (n is large enough for a such approximation since n={88,97,74,259}). We then use the statistical test of Azais & Genz (2013) and consider the centered process :

$$M_X(t) = m_X(t)-\mu, \text{ with } t=\{1,2, ... 24\} \text{ half an hours,}$$

where μ is the mean killing each half an hours of the whole population during all the experiment. Recall that mathematically, μ is given by :

$$\mu = (m_X(1)+m_X(2)+...+m_X(24)) / 24.$$

Then, we compute for any time s between 1 and 24 half an hours the mean killing per unit of time before and after s. These two averages are thus :

$$M_-(s) = (m_X(1)+m_X(2)+...+m_X(s-1)) / (s-1),$$

and :

$$M_+(s) = (m_X(s+1)+m_X(s+2)+...+m_X(24)) / (24-(s+1)) .$$

To test the change in the mean of the time series, the difference between these two averages is a key mathematical ingredient, which must be normalized by the variance of the averaging before and after time s :

$$\Delta(s)=|M_-(s)-M_+(s)| / (\sqrt{(s-1)}+\sqrt{(24-(s+1))}.$$

The change in the mean test relies on the maximum of ($\Delta(s)$, $1<s<24$). Following standard notations of extreme events theory, this maximum is denoted M^*.

Let us denote now H_0 the baseline assumption that no breakpoint in the mean occur in the time series ($X(t)$, $0 < t < 25$), the statistical procedure relies on the value M^*: under the assumption that X follows a centered GP, the distribution of the random variable M^* can be

computed and especially the probability that M^* is greater than a given threshold u: $P(M^* > u)$ by using an intricate and very effective Quasi Monte Carlo integration, which is described by Genz (2012).

We then compute the observed statistics M^* in each of our situation and decide to reject the baseline hypothesis H_0 each time the p-value is lower than 5%. Using the Matlab package and the `qsimvnv` function, we obtained the following numerical results :

- The first data subset made up of 88 CTL killing kinetics presents a change in the average behavior of the CTL and the first type error of our test is lower than $p_{value}=1.5\ 10^{-4}$, (meaning that our statistics would occur with a probability lower than p_{value} if no breakpoint occurs in the series). Moreover, this breakpoint is likely to occur at about 8.5 hr.
- The second data subset made up of 97 CTL killing kinetics is associated to a first type error test lower than $p_{value}=8.9\ 10^{-4}$ with a breakpoint likely to occur at about 10 hr.
- The third data subset made up of 74 CTL killing kinetics is associated to a first type error test lower than $p_{value}=5.7\ 10^{-4}$ with a breakpoint likely to occur at about 10 hr.
- The compiled dataset comprising 259 CTL killing kinetics is associated to a first type error test lower than $p_{value}=5.7\ 10^{-4}$ with a breakpoint likely to occur at about 10 hr.

Whatever the data set considered, our statistical analysis leads to the rejection of the homogeneity in the time series. Note also that we have decided to pinpoint the breakpoint location at the time where $\Delta(s)$ reaches its maximal value.

References

Azais & Genz (2013) Computation of the Distribution of the Maximum of Stationary Gaussian Processes. Methodology and Computing in Applied Probability, 15:969-985.

Rychlik (1990) New bounds for the first passage, wavelength and amplitude density. Stochastic Processes and their Applications, 34:313–339.

Genz (2012) Matlab software for multivariate normal probability computations. www.math.wsu.edu/faculty/genz/software/software.html

Figure S1

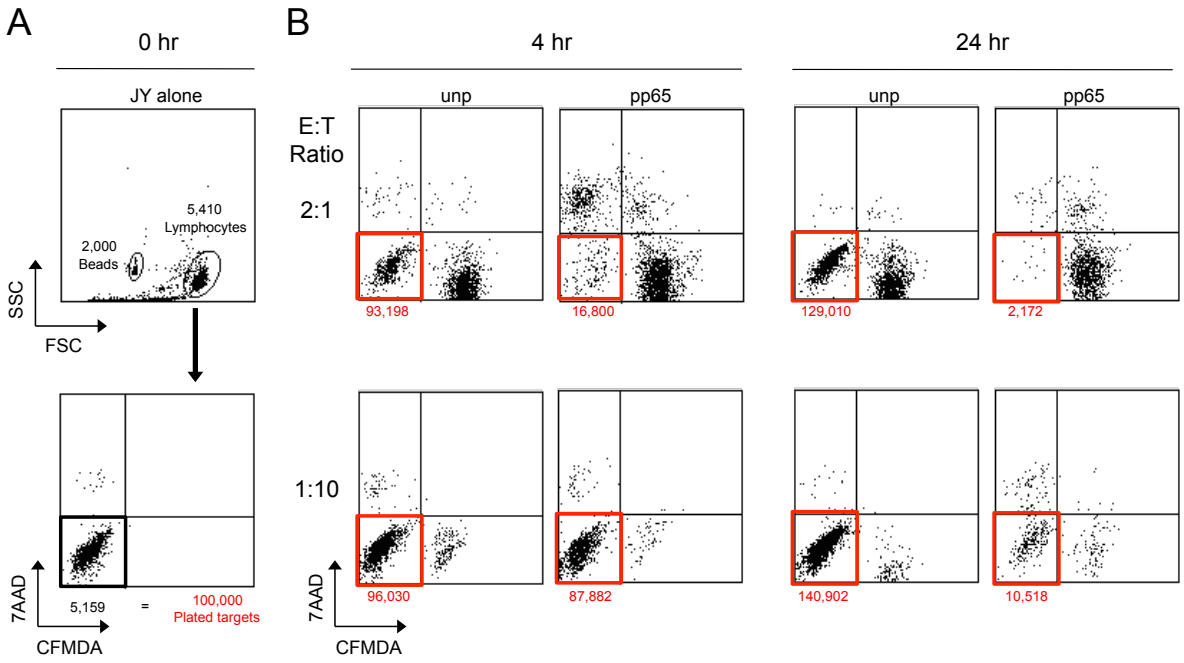

Figure S1, Related to Figure 1. Flow cytometry-based counting of alive target cells
JY cells (Targets) were pulsed with 100 nM pp65 or left unpulsed and co-cultured for 4 and 24 hr with CTL (Effectors), at E:T ratios of 2:1 and 1:10. Before flow cytometry analysis, microbeads were added to harvested cells to serve as internal control. (**A**) The upper left dot plot corresponds to the reference tube containing JY cells only, which was acquired until a number of 2,000 beads was reached. The lower left dot plot indicates how alive target cells were discriminated (7AAD negative and CFMDA negative) to establish a reference count corresponding to the initial 100,000 cells used. (**B**) Tubes corresponding to the indicated experimental conditions were also acquired until a number of 2,000 beads was reached. The 7AAD/CFMDA plots allow to discriminate target cells (CFMDA negative) from CTL (CFMDA positive) and alive cells (7AAD negative) from dead ones (7AAD positive). The numbers of alive target cells were calculated on the basis of the reference tube. The plots are from one representative experiment.

Figure S2

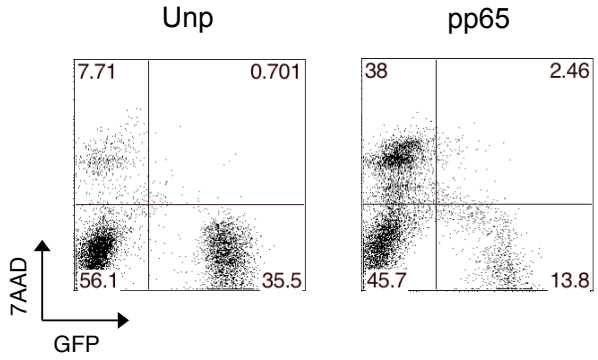

Figure S2, Related to Figure 2. Loss of GFP in target cells as a measurement of death
GFP-expressing target cells, pulsed with 100 nM pp65 or left unpulsed, were co-cultivated with CTL at a 2:1 E:T ratio for 4 hr and subsequently analyzed by flow cytometry for GFP expression and 7-AAD staining. CTL-mediated killing of target cells results in a loss of GFP, which is concomitant to 7-AAD uptake. Dot plots are representative of 3 experiments.

Figure S3

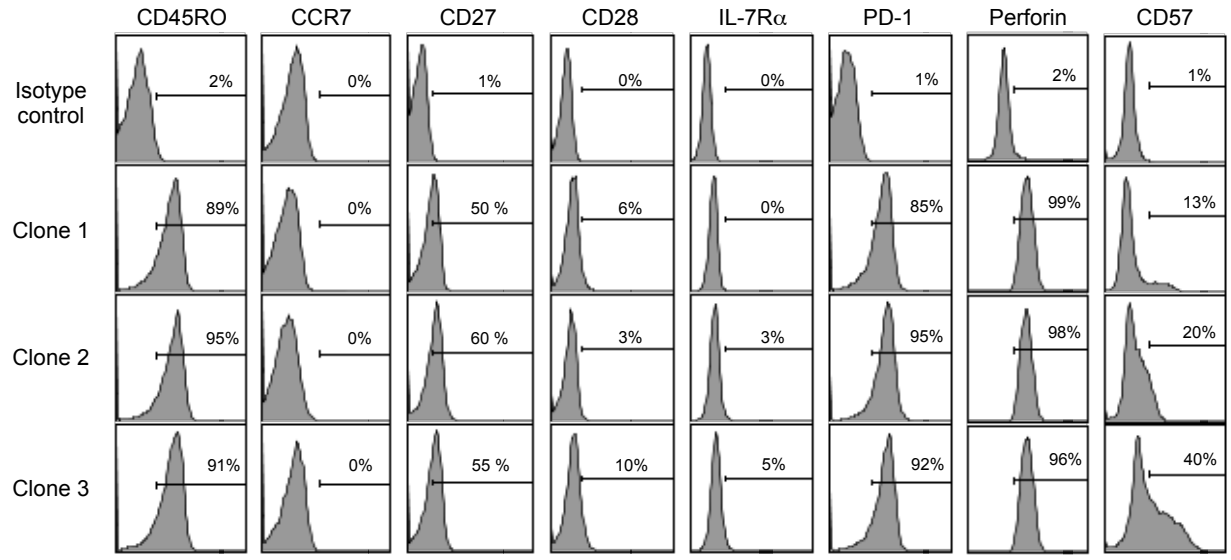

Figure S3, Related to Figure 2. Homogenous effector memory phenotype in the pp65-specific CTL clones

Representative flow cytometry analysis of the phenotype of three pp65-specific $CD8^+$ CTL clones, based on the expression of CD45RO, CCR7, CD27, CD28, CD127 (IL-7Rα), PD-1, Perforin and CD57.

Figure S4

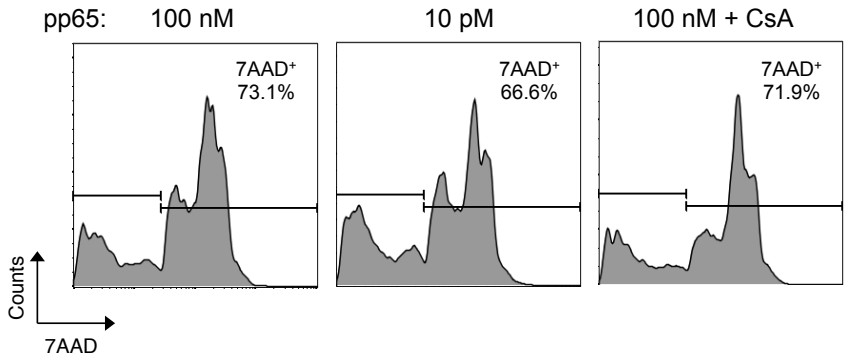

Figure S4, Related to Figure 7. Early CTL cytotoxicity under reduced activation conditions
CTL were incubated with JY cells pulsed with 100 nM or 10 pM pp65 at a 2:1 E:T ratio during 4 hr in the presence or absence of 1 μg/mL CsA. Histogram plots showing percentage of target cells positive for 7-AAD are representative of 3 experiments.

Movie S1, Related to Figure 3. Rapid cumulative rise in caspase-3-positive target cells at 1:1 E:T ratio
Representative wide field of a Lab-Tek well showing the activation of Caspase-3 (with NucView 488 caspase-3 substrate) in JY target cells pulsed with 100 nM pp65 and incubated with specific CTL at a 1:1 E:T ratio. Images were taken over 12 hr at a frame rate of 1 image every 2 min.

Movie S2, Related to Figure 3. Substantial but delayed rise in caspase-3-positive target cells at 1:10 E:T ratio
Representative wide field of a Lab-Tek well showing the activation of Caspase-3 (with NucView 488 caspase-3 substrate) in JY target cells pulsed with 100 nM pp65 and incubated with specific CTL at a 1:10 E:T ratio. Images were taken over 12 hr at a frame rate of 1 image every 2 min.

Movie S3, Related to Figure 3. Low activation of caspase-3 in unpulsed target cells
Representative wide field of a Lab-Tek well showing the activation of Caspase-3 (with NucView 488 caspase-3 substrate) in unpulsed JY target cells incubated with specific CTL at a 1:1 E:T ratio. Images were taken over 12 hr at a frame rate of 1 image every 2 min.

Movie S4, Related to Figure 4. High-rate multiple killing by a single CTL
Selected microwell of a PDMS micromesh array showing a single CTL (prestained with CellTrace™ Calcein Red-Orange) displaying high cumulative killing, as evidenced by activation of Caspase-3 (with NucView 488 caspase-3 substrate) in multiple JY target cells pulsed with 100 nM pp65.

Movie S5, Related to Figure 4. Low-rate multiple killing by a single CTL
Selected microwell of a PDMS micromesh array showing a single CTL (prestained with CellTrace™ Calcein Red-Orange) displaying low cumulative killing, as evidenced by activation of Caspase-3 (with NucView 488 caspase-3 substrate) in few JY target cells pulsed with 100 nM pp65.

Movie S6, Related to Figure 4. Low activation of caspase-3 in the absence of CTL
Selected microwell of a PDMS micromesh array showing background activation of Caspase-3 (with NucView 488 caspase-3 substrate) in JY target cells pulsed with 100 nM pp65, in the absence of CTL.